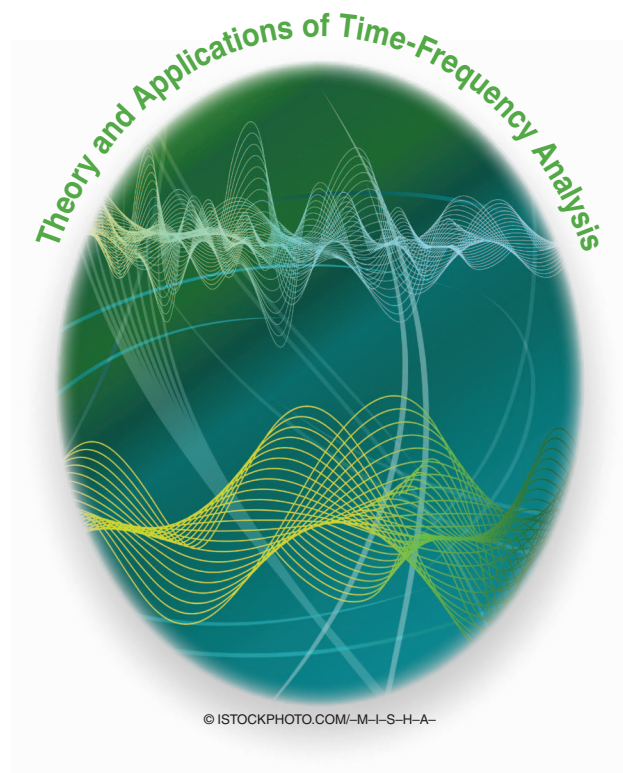François Auger, Patrick Flandrin, Yu-Ting Lin, Stephen McLaughlin,
Sylvain Meignen, Thomas Oberlin, and Hau-Tieng Wu

Time-Frequency Reassignment and Synchrosqueezing

Theory and Applications of Time-Frequency Analysis

© ISTOCKPHOTO.COM/–M–I–S–H–A–

[An overview]

This article provides a general overview of time-frequency (T-F) reassignment and synchrosqueezing techniques applied to multicomponent signals, covering the theoretical background and applications. We explain how synchrosqueezing can be viewed as a special case of reassignment enabling mode reconstruction and place emphasis on the interest of using such T-F distributions throughout with illustrative examples.

INTRODUCTION

Over the last 30 years, numerous methods have been proposed to extend Fourier analysis to nonstationary signals, resulting in a body of work that is referred to (at large) as T-F methods [1]–[3]. Broadly speaking, generalizing Fourier analysis to take into account possible variations in the frequency
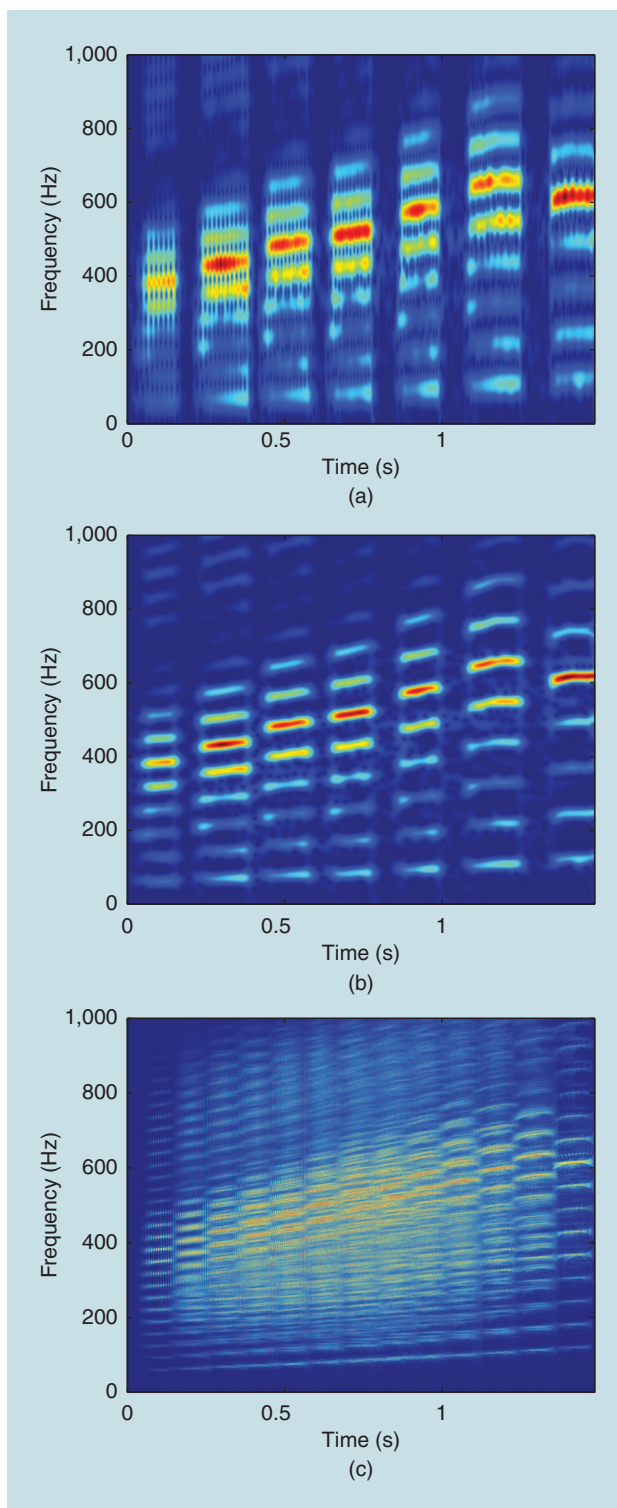
content of a signal can be understood in two complementary ways. The first attempts to make the Fourier transform time dependent, while the second focuses on the associated spectral density. The main difference is that the first approach is linear, with a complex-valued frequency description that involves magnitude and phase contributions, whereas the second is quadratic and leads to real-valued transforms in most cases.

Linear T-F methods include short-time Fourier transforms (STFTs) and wavelet transforms (WTs), while most quadratic methods can be seen as variations of the celebrated Wigner–Ville distribution (WVD), with squared STFTs (spectrograms) and WTs (scalograms) as special cases. Perhaps the key point is that none of these approaches allow for the definition of one and only one transform. This follows in some sense from the uncertainty relation that links time and frequency, with the consequence that the result of any transform depends not only on intrinsic characteristics of the analyzed signal, but also on the specific properties of the chosen transform; i.e., the transform should be viewed as a measurement device. In the case of linear methods, this entanglement between the measured quantity and the measuring device takes on a special importance when, e.g., the signal under study is almost as elementary (in terms of Heisenberg–Gabor uncertainty) as the window or wavelet used for its analysis: in such a situation, one could think of the signal analyzing the window as much as the window analyzing the signal! Something similar occurs for AM–FM signals: while the idealized picture of such signals would correspond to perfectly localized trajectories associated with the instantaneous frequencies in the T-F plane, values of linear transforms are spread over a ribbon whose geometry depends jointly on the signal and the window (see Figures 1 and 2).

To overcome this difficulty, in the late 1970s, Kodera et al. pioneered an approach aimed at "modifying" the "moving window method" (i.e., the STFT) [4], [5]. Their analysis pointed out that the spreading of the STFT magnitude (the quantity that is usually displayed in graphical representations) can be compensated by taking into account the phase information that is usually discarded. This offered a dramatic improvement in terms of readability, but because no inversion formula exists, this approach did not receive much attention.

Subsequently, in the 1980s, came the development of Wigner-type distributions that could be tailored to guarantee perfect localization of signals with specific FM laws (linear for the Wigner distribution and, e.g., hyperbolic for some of its generalizations), though at the expense of new difficulties, e.g., cross-terms that hampered readability in the multicomponent case. Nevertheless, this new way of interpreting squared linear transforms permitted a revisit of Kodera's approach and an extension of its applicability beyond the STFT. Moreover, Auger and Flandrin (who coined the term *reassignment*) showed in the early 1990s that the explicit use of the STFT phase can be efficiently replaced by a combination of STFTs with suitable windows [6]. This was the starting point of its use in a variety of new domains, such as audio [7], physics [8], or ecology [9].

[FIG1] An illustration of the Heisenberg uncertainty principle: a spectogram of a saxophone sound computed with Gaussian windows (a) σ=9 ms and (b) σ=15 ms. (c) WVD of the saxophone sound.

In parallel (and independently), Maes and Daubechies developed another phase-based technique that they termed *synchrosqueezing* [10]. Its purpose was very similar to that of reassignment (indeed it is a special case), with the

additional advantage of allowing for reconstruction.

The late 1990s saw the introduction of a radically different proposal with empirical mode decomposition (EMD) [11], designed to extract AM–FM components in a data-driven manner. Though attractive due to its simplicity and effectiveness, EMD lacked solid mathematical foundations. In this context, synchrosqueezing has recently resurfaced as a more formalized alternative [12] as well as an appealing technique [13]. Reassignment has, in turn, received new attention [14], and the purpose of this article is to offer a brief guided tour emphasizing key features of both techniques, clarifying their relationships, and illustrating them with some example applications.

NOTATION AND MULTICOMPONENT SIGNAL DEFINITION

Let us first define the notation that will be used throughout the article. Given a signal $f \in L^1(\mathbb{R})$, the space of integrable functions, and taking a window g in the Schwartz class, the space of smooth functions with fast decaying derivatives of any order, the STFT of f is defined by

$$V_f^g(t, \omega) = \int_{\mathbb{R}} f(\tau) g^*(\tau - t) e^{-i\omega\tau} d\tau, \qquad (1)$$

where $g^*(t)$ is the complex conjugate of $g(t)$. The spectrogram $S_f^g(t, \omega)$ is then usually defined as $|V_f^g(t, \omega)|^2$. One of the most popular cases is when g is the Gaussian window $1/\sqrt{2\pi}\,\sigma\,e^{-t^2/2\sigma^2}$. Multicomponent signals f to be considered in either reassignment or synchrosqueezing techniques in the STFT framework are defined by

$$f(t) = \sum_{k=1}^{K} f_k(t), \quad \text{with } f_k(t) = a_k(t) e^{i\phi_k(t)} \qquad (2)$$

for some finite K, where $a_k(t) > 0$ is a continuously differentiable function, ϕ_k is a two times continuously differentiable function satisfying $\phi_k'(t) > 0$ and $\phi_{k+1}'(t) > \phi_k'(t)$ for all t. In the following, $f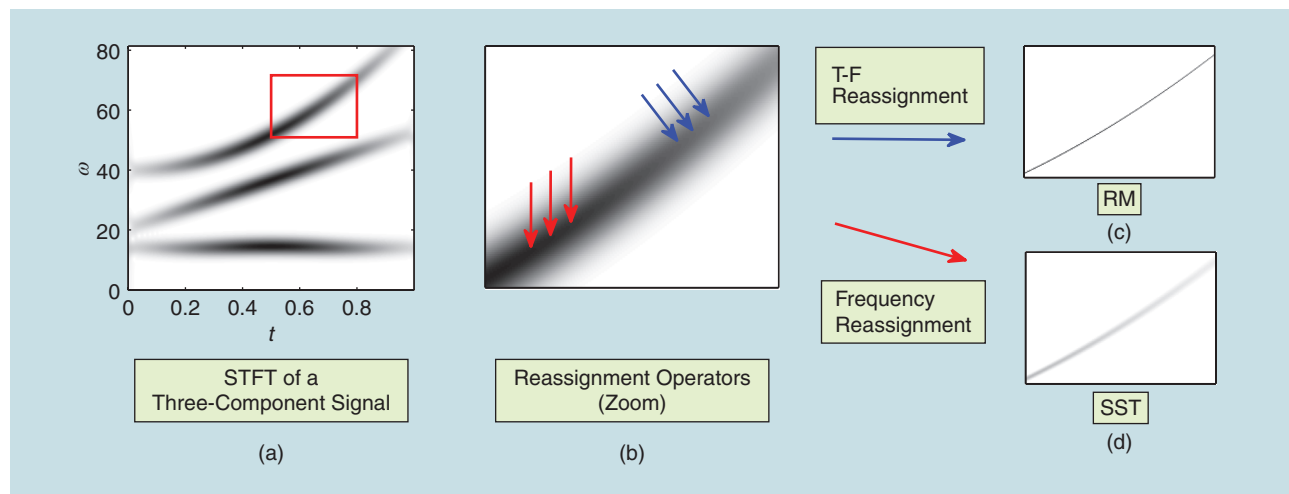_k$ will be referred to as an AM–FM component or a mode of f. In that context, ideal T-F (ITF) representations can be defined as

$$\text{ITF}_q(t, \omega) = \sum_{k=1}^{N} a_k(t)^q \delta(\omega - \phi_k'(t)), \qquad (3)$$

where q is a positive integer depending on the chosen T-F distribution (TFD), the STFT (respectively spectrogram) being associated with $q = 1$ (respectively $q = 2$). In that context, $\phi_k'(t)$ is called the instantaneous angular frequency (IAF) of the kth mode at time t.

UNCERTAINTY PRINCIPLE FOR MULTICOMPONENT SIGNALS

The most significant issue in T-F signal analysis is the uncertainty principle, which stipulates that one cannot localize a signal with an arbitrary precision both in time and frequency. T-F representations often include parameters to allow for the balance between frequency resolution and time localization. In the case of the STFT (or spectrogram), this can be achieved by varying the size of the analysis window. As an illustration, we display the spectrogram of a saxophone's sound (i.e., a succession of several notes) for two sizes of the window g in Figure 1(a) and (b): a small window localizes the transients well (the beginning of each note), while a large one gives precise frequency information. There have been many attempts to optimize this tradeoff, among which are the WVD, other quadratic representations from the Cohen's class [1], [2], and multilinear distributions

[FIG2] (a) A three-component signal STFT modulus. (b) Blue (respectively red) arrows symbolizing how the reassignment is performed with RM (respectively SST) on a small patch (delimited by the red segments) extracted from representation (a). (c) Reassignment carried out with RM for the signal STFT depicted in (b). (d) The same as (c) but using the SST.

(see [15], for instance). However, improvements in terms of T-F resolution brought about by these techniques usually rely on strong assumptions so that each method is suited only for a specific class of signals.

TIME-FREQUENCY REPRESENTATION ENHANCEMENT WITH REASSIGNMENT

Reassignment techniques offer an alternative approach. They aim to sharpen the T-F representation while keeping the temporal localization and are particularly well adapted to multicomponent signals. Starting with the definition (1) of the STFT, the spectrogram can be written as [1]

$$S_f^g(t, \omega) = \frac{1}{2\pi} \iint_{\mathbb{R}^2} W_g(\tau - t, \nu - \omega) W_f(\tau, \nu) \, d\tau \, d\nu, \quad (4)$$

where $W_f(t, \omega)$ is the WVD, defined for any f in $L^2(\mathbb{R})$ by

$$W_f(t, \omega) := \int_{\mathbb{R}} f(t + \tau/2) f^*(t - \tau/2) e^{-i\omega\tau} \, d\tau. \quad (5)$$

The spectrogram is thus the two-dimensional (2-D) smoothing of the WVD of the analyzed signal by the WVD of the analyzing window. This alternative formulation allows for a simple understanding of the main features of a spectrogram when compared to a WVD. On the one hand, a WVD is known to sharply localize individual linear chirps in the T-F plane but the 2-D smoothing involved in the spectrogram computation results in a smearing of their energy distribution. On the other hand, the quadratic nature of the WVD is known to create oscillatory interference between individual components ([3, Ch. 3] [see Figure 1(c) for an illustration], which can be removed by the 2-D smoothing used in the spectrogram computation. The analysis is therefore faced with a tradeoff between T-F localization and the interference level.

From (4), it follows that the value of the spectrogram at (t, ω) is the sum of all WVD signal contributions within the T-F domain over which the WVD of the window is essentially nonzero. The principle of the reassignment method (RM) illustrated here on the spectrogram is to compensate for the T-F shifts induced by the 2-D smoothing defining the spectrogram. To do so, a meaningful T-F location to which to assign the local energy given by the spectrogram is first determined. It corresponds to the centroid of the distribution (4), whose coordinates are defined by

$$\hat{\omega}_f(t, \omega) := \frac{1}{S_f^g(t, \omega)} \iint_{\mathbb{R}^2} \nu \, W_g(\tau - t, \nu - \omega) W_f(\tau, \nu) \frac{d\tau \, d\nu}{2\pi}$$

$$\hat{t}_f(t, \omega) := \frac{1}{S_f^g(t, \omega)} \iint_{\mathbb{R}^2} \tau \, W_g(\tau - t, \nu - \omega) W_f(\tau, \nu) \frac{d\tau \, d\nu}{2\pi}.$$

Both quantities, which define locally an instantaneous frequency and a group delay, enable perfect localization of linear chirps, i.e., $\phi'(\hat{t}_f(t, \omega)) = \hat{\omega}_f(t, \omega)$. RM then consists of moving the value of the spectrogram from the point of computation to this centroid [6]

$$\hat{S}_f^g(t, \omega) = \iint_{\mathbb{R}^2} S_f^g(\tau, \nu) \, \delta(\omega - \hat{\omega}_f(\tau, \nu))$$
$$\delta(t - \hat{t}_f(\tau, \nu)) \, d\tau \, d\nu, \quad (6)$$

where δ stands for the Dirac distribution. Due to the above mentioned property of $(\hat{t}_f(t, \omega), \hat{\omega}_f(t, \omega))$, RM perfectly localizes linear chirps while removing most of the interference. However, in practice, the centroid $(\hat{t}_f, \hat{\omega}_f)$ is not evaluated as above. A more efficient [6] procedure computes it according to

$$\hat{\omega}_f(t, \omega) = \omega - \Im\left\{\frac{V_f^{g'}(t, \omega)}{V_f^g(t, \omega)}\right\} \quad (7)$$

$$\hat{t}_f(t, \omega) = t + \Re\left\{\frac{V_f^{tg}(t, \omega)}{V_f^g(t, \omega)}\right\}, \quad (8)$$

where tg stands for the function $tg(t)$ and $\Re\{Z\}$ (respectively $\Im\{Z\}$) is the real (with respect to an imaginary) part of the complex number Z. Compared to the standard spectrogram, its reassigned version can thus be computed with a moderate increase in the computational cost since three STFTs are evaluated (and combined) instead of one. An illustration of RM is given in Figure 2(c). In this regard, when the analysis window is Gaussian, the centroid can also be computed from the STFT magnitude [16] or alternatively be defined by means of time and frequency partial derivatives of the phase of $V_f^g(t, \omega)$ [4], [5].

The advantage of revisiting RM is that it enables the extension of the principle of reassignment defined here on the spectrogram to any distribution that results from some form of smoothing applied to a "mother-distribution" that has localization properties for specific chirps [3]. Indeed, the above presentation can be easily generalized by replacing in (4) W_g by some other kernel Π attached to a distribution within Cohen's class to obtain

$$\tilde{S}_f^g(t, \omega) = \frac{1}{2\pi} \iint_{\mathbb{R}^2} \Pi(\tau - t, \nu - \omega) W_f(\tau, \nu) \, d\tau \, d\nu.$$

The general requirements imposed on such TFDs is that they preserve the signal energy, their local extrema in frequency are good estimates of the IAF of the components, robust to noise, and the signal energy is mainly concentrated in the vicinity of these local extrema. A potentially interesting TFD is given by the modified B-distribution defined as above with $\Pi(t, \nu) = (k/\cosh^{2\beta}(t)) \delta(\nu)$, k being a normalization constant. When β is optimally chosen, this technique may outperform other TFDs in terms of T-F resolution and cross-terms suppression when used to represent signals with closely spaced components in the T-F domain [17]. Other distributions like the S-method generalizes the spectrogram by considering $\Pi(t, \nu) = p(t) W_g(t, \nu)$, where p is some time

> **WHILE RM PROVIDES A DIRECT AND POWERFUL REPRESENTATION OF A MULTICOMPONENT SIGNAL IN THE T-F PLANE, NO MODE RECONSTRUCTION TECHNIQUE USING THE REASSIGNED TRANSFORM IS STRAIGHTFORWARD.**

window whose choice determines the quality of the representation [18].

SEPARATION OF COMPONENTS WITH CLOSE IAF IS A COMMON PROBLEM IN TIME SERIES OR BIOMEDICAL SIGNAL ANALYSIS.

MULTICOMPONENT SIGNAL RECONSTRUCTION WITH SYNCHROSQUEEZING

While RM provides a direct and powerful representation of a multicomponent signal in the T-F plane, no mode reconstruction technique using the reassigned transform is straightforward. In contrast, the synchrosqueezing transform (SST), introduced by Maes and Daubechies in [10], enhances the TFD given by the STFT in a manner similar to RM with the spectrogram, but it still enables mode retrieval as in EMD [11]. This property is of great importance since the understanding of a multicomponent signal as defined in (2) is tightly related to the analysis of its constituent modes. Furthermore, in contrast to EMD, mode reconstruction using SST is carried out in a convenient mathematical framework. Indeed, a recent result [12] shows that the SST is a good approximation to the ITF representation of the signal f [with $q = 1$; see (3)] and enables mode reconstruction when f is made of weakly modulated modes. We now present the SST in the STFT framework with the emphasis on the differences with RM providing insights into some theoretical results.

SST IN A NUTSHELL

In contrast to RM, which enhances the TFD given by the spectrogram, the SST operates directly on the STFT. The construction of the SST is closely related to the synthesis formula

$$f(t) = \frac{1}{2\pi g(0)^*} \int_{\mathbb{R}} V_f^g(t, \omega) e^{i\omega t} \, d\omega, \qquad (9)$$

which sums the STFT in frequency for each time t. However, when f is made of separate components f_k in the T-F plane, i.e., verifying (2) and conditions (13) and (14), the main part of the STFT of f_k is localized in the vicinity of the ridge $(t, \phi_k'(t))$, which can be seen as the T-F trajectory associated with component k. The interesting angular frequencies (AFs) ω used to reconstruct f_k are then selected as those such that $\hat{\omega}_f(t, \omega)$ is a good approximation of $\phi_k'(t)$ [19]. Based on this idea, the synchrosqueezing operator reassigns the STFT as follows:

$$T_f^g(t, \omega) = \frac{1}{2\pi g(0)^*} \int_{\mathbb{R}} V_f^g(t, \nu) e^{i\omega t} \delta(\omega - \hat{\omega}_f(t, \nu)) \, d\nu. \quad (10)$$

Note that this definition is similar to that used by RM, except that time reassignment is not considered and V_f^g is used instead of the spectrogram [an illustration of what the operator T_f^g does is given in Figure 2(d)]. It is interesting to note that a dual operator was introduced in [18] by considering time reassignment instead of frequency reassignment. However since this was carried out on the spectrogram rather than on the STFT it did not allow for mode reconstruction.

Having computed the synchrosqueezing operator T_f^g, the kth mode is then reconstructed by integrating T_f^g in the vicinity of the corresponding ridge

$$f_k(t) \approx \int_{\{\omega, |\omega - \phi_k'(t)| < d\}} T_f^g(t, \omega) \, d\omega, \qquad (11)$$

for some small parameter d. Since $\phi_k'(t)$ is unknown and needs to be estimated in practice, this local averaging of T_f^g in frequency (t being fixed) is compulsory to retrieve f_k.

Given T_f^g and assuming the number K of components is known, a ridge extraction technique can be used to estimate the ϕ_k's before proceeding with mode retrieval. For this, there exists a variety of methods [20], [21], but those based on ridge estimation are particularly well adapted to the SST case. Briefly, the principle of the latter techniques is to minimize the following energy functional initially proposed by Carmona et al. [22]:

$$E_f(\varphi) = \sum_{k=1}^{K} - \int_{\mathbb{R}} | T_f^g(t, \varphi_k(t)) |^2 \, dt + \int_{\mathbb{R}} \lambda \varphi_k'(t)^2 + \beta \varphi_k''(t)^2 \, dt. \qquad (12)$$
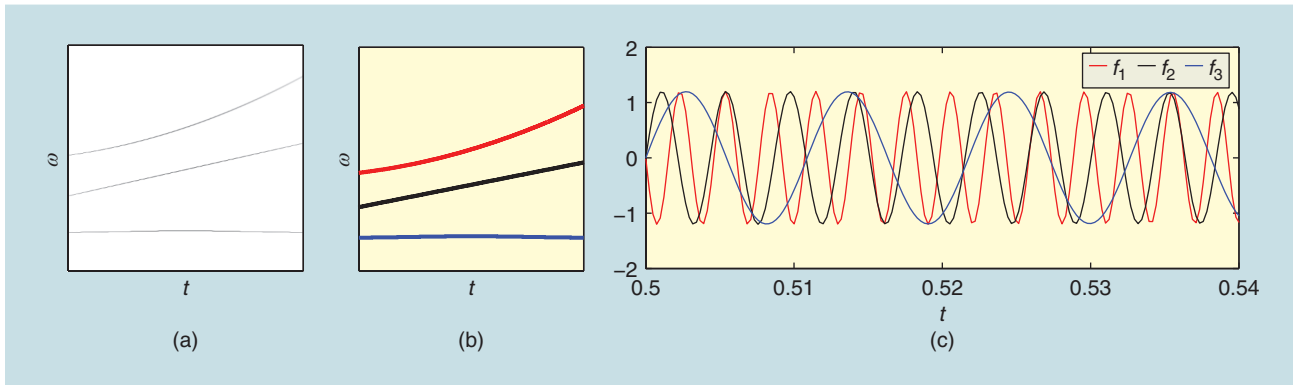
Doing so, one finds smooth curves φ_k along which the magnitude of T_f^g is maximal, λ and β enabling a tradeoff between smoothness of the curve and energy maximization. Although this general variational formulation looks very appealing, it is hard to implement. Heuristic algorithms such as simulated annealing [22] or the crazy climbers algorithm [23], which are particularly appropriate in a noisy context, have to be used. Another simple yet efficient approach related to the resolution of (12) was developed in [24] and consists of a local determination of the ridges starting from different initializations and then in an averaging of the results obtained. All these three methods behave very similarly on the examples studied, and the illustrative examples that follow will use the last method as ridge estimator. A summary of how the SST performs mode retrieval is given in Figure 3. To conclude, it is worth noting here alternative approaches that assume a polynomial phase for the modes [25], whereas the SST does not require such an assumption.

MATHEMATICAL FOUNDATIONS OF THE SST

The discussion above on mode retrieval is reinforced by some theoretical results mostly derived in the wavelet framework in [12] and then adapted to the STFT context in [19]. Our goal here is not to delve too deeply into the derivation of these results, but to focus on what type of signals for which they are valid. They are obtained under the following assumptions on the signal f, assuming the window g is Gaussian:

A1) the f_ks have weak frequency modulation, implying the existence of a small ε such that for each t, one has

$$\sigma^2 | \phi_k''(t) | \le \varepsilon \text{ and } | a_k'(t) | \le \varepsilon \phi_k'(t), \qquad (13)$$

[FIG3] (a) The SST modulus. (b) Ridge extraction from SST. (c) Mode retrieval based on ridge extraction.

where σ is the size of the Gaussian window.

A2) The modes are well separated in frequency, which corresponds, assuming the frequency bandwidth of g (in rad/s) is $[-\Delta, \Delta]$ ($\Delta = \sqrt{2\log(2)}/\sigma$ since g is the Gaussian window), to an inequality of type

$$|\phi'_k(t) - \phi'_l(t)| \geq 2\Delta \tag{14}$$

for each t and $k \neq l$.

Note that because the modes f_k are such that $\phi'_k(t) < \phi'_{k+1}(t)$ for all t, (14) can always be satisfied by choosing a Gaussian window with the appropriate size. A mode f_k satisfying A1) will be called an $\mathcal{A}_\varepsilon$ signal later in the article. Under these hypotheses, one has that

1) for any (t, ω) in $\bigcup_k \{(t, \omega); |\omega - \phi'_k(t)| \leq \Delta\} = \bigcup_k B_k$, there exists a k such that $|\hat{\omega}_f(t, \omega) - \phi'_k(t)| \leq C\varepsilon$, where C is some constant

2) the reconstruction error associated with the retrieval of f_k by summing the coefficients around $T^g_f(t, \phi'_k(t))$ following (11) tends to zero as ε goes to zero.
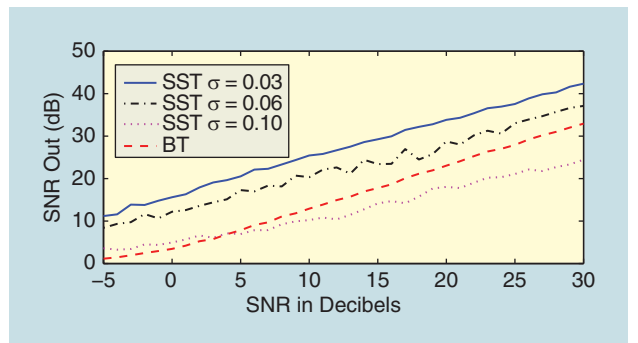
This clearly establishes, on one hand, the relation between the amplitude of ε and the quality of the modes retrieval and, on the other hand, the role played by the window's size in the separation of the components.
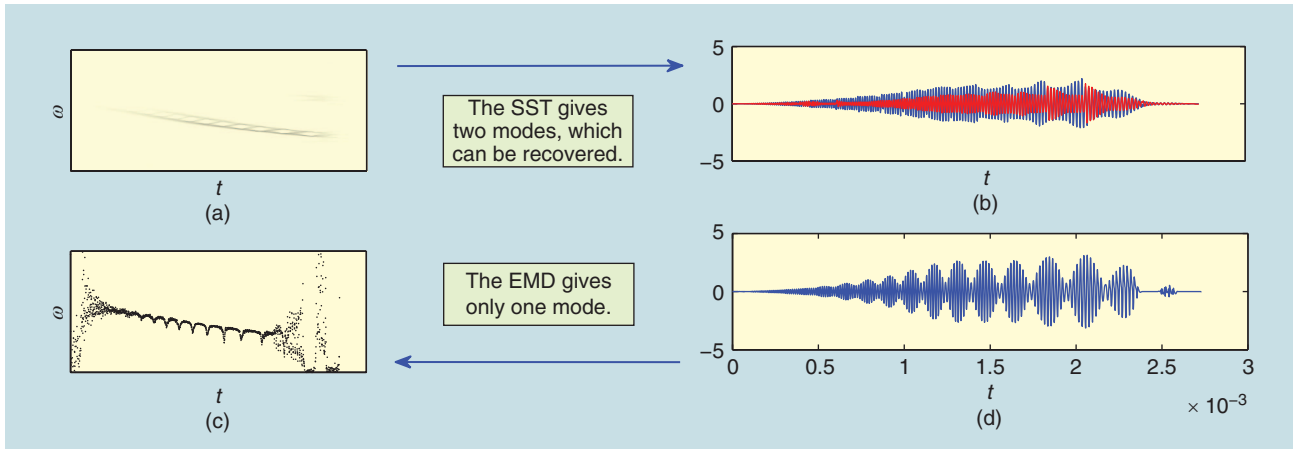
ILLUSTRATIONS OF THE SST

DENOISING MULTICOMPONENT SIGNALS USING SST

Here we here illustrate how the SST provides us with a naive denoising procedure that can outperform a state-of-the-art method based on wavelets. To do so, we consider the signal whose STFT is shown in Figure 2(a) to which we add white Gaussian noise with varying standard deviation, leading to different SNR (SNR in). Then we denoise this signal with the block-thresholding (BT) method developed in [26], a T-F technique designed for audio recordings, and also with the SST, by simply selecting three ridges as explained in the section "SST in a Nutshell" (with $\lambda = 0$ and $\beta = 0.02$; these parameters, though not optimal, lead to good results in practice). The results displayed in Figure 4

in terms of the SNR before and after denoising (SNR in and out, respectively, the SNR out being computed as $\|f\|^2/\|f - \tilde{f}\|^2$, where $\tilde{f}$ is the denoised signal) show a much better denoising performance of the SST over BT on this particular example, provided σ is appropriately chosen. As soon as the ridges are detected, the SST thus enables signal denoising in a straightforward manner. However, when the signal contains highly modulated modes, as in the studied case, the use of too large a window should be proscribed, as is reflected by the first inequality of (13). In this regard, we will later try to go beyond this limitation by taking into account the modulation in the synchrosqueezing operator. It is also noteworthy that, as the modes are not perfectly monochromatic, their SST is not perfectly reassigned onto the ridges. In this regard, the parameter d introduced in the reconstruction formula (11) enables compensation for the lack of accuracy in the estimation of $\phi'_k(t)$ by means of $\hat{\omega}_f(t, \omega)$. It has to be chosen all the larger that the modulation is important ($d = 8$ rad/s being satisfactory in the studied case). Finally, we remark that by considering modified versions of the spectrogram one could obtain better ridge estimations than with the SST in such a noisy context [18]. However, in doing so, the reconstruction properties inherent to the SST would be lost.

[FIG4] The denoising performance with the SST and BT techniques for the signal whose STFT is depicted in Figure 2(a) and for various window's size σ, d being fixed to 8 rad/s.

[FIG5] (a) The modulus of the STFT of a bat echolocation call. (b) Modes computed using the SST from representation (a). (c) Hilbert spectrum of the mode displayed in (d). (d) Mode computed with the EMD.

MODE SEPARATION: SST VERSUS EMD

Separation of components with close IAF is a common problem in time series or biomedical signal analysis. EMD, introduced in [11], aims at decomposing a multicomponent signal s into modes h_j, $1 \le j \le J$, $f(t) = \sum_{j=1}^{J} h_j(t) + r(t)$, where the h_js oscillate decreasingly with increasing j, and r is a monotonic residue. In this context, h_j is defined as a locally oscillating function having a symmetric envelope and is computed by subtracting to m_{j-1} its mean envelope, m_{j-1} being defined by

$$ m_{j-1}(t) = \begin{cases} f(t), & j = 1 \\ f(t) - \sum_{i=1}^{j-1} h_i(t), & j > 1. \end{cases} $$

The separation power of EMD was studied in [27] and depends on the amplitude and frequency ratio between the modes: if they are too close, EMD cannot separate them. In the case of the SST, by choosing the bandwidth of g appropriately, one can obtain mode separation in instances where the EMD cannot, which confers a greater flexibility. As an illustration, we consider a bat echolocation call containing two modes with close IAFs ϕ'_k. We display in Figure 5(a) the modulus of the STFT (computed using a Gaussian window with $\sigma = 0.08$ ms) and the two extracted components using SST [Figure 5(b)]. The Hilbert–Huang spectrum [11] corresponding to the first mode obtained with EMD and that mode are displayed in Figure 5(c) and (d), respectively. While SST shows two distinct components that are well detected and reconstructed using formula (11), EMD instead considers the signal as a single modulated mode.

NEW DEVELOPMENTS AND PERSPECTIVES ON REASSIGNMENT AND SYNCHROSQUEEZING

ADJUSTABLE REASSIGNMENT

Since the initial publications, many extensions and applications of RM have been proposed. Recently, a variant of RM, referred to as the *Levenberg–Marquardt reassignment*, was presented in [14]. This technique gathers the values of the spectrogram around the ridges of the signal, which are viewed as the zeros of the relative displacement operator

$$ R_f^g(t, \omega) := (t - \hat{t}_f(t, \omega), \omega - \hat{\omega}_f(t, \omega))^T, \qquad (15) $$

where X^T is the transpose of vector X. To find out an approximation $(\tilde{t}_f(t, \omega), \tilde{\omega}_f(t, \omega))$ of the centroid $(\hat{t}_f(t, \omega), \hat{\omega}(t, \omega))$, a root-finding algorithm known as the Levenberg–Marquardt method is used

$$ (\tilde{t}_f(t, \omega), \tilde{\omega}_f(t, \omega))^T = (t, \omega)^T - (J(R_f^g)(t, \omega) + \mu I_2)^{-1} R_f^g(t, \omega), \qquad (16) $$

where $J(R_f^g)(t, \omega)$ is the Jacobian matrix of $R_f^g(t, \omega)$ and I_2 the 2×2 identity matrix. Note that this algorithm can be interpreted as an iteration of a Newton-like method (when $\mu = 0$ the true Newton method is obtained, which corresponds to a first-order approximation of the ridge). Then, by using the new centroid $(\tilde{\omega}_f(t, \omega), \tilde{t}_f(t, \omega))$, a new reassigned spectrogram can then be defined following the framework of (6). The main characteristic of this new reassigned representation is the extra parameter μ allowing the user to tune the representation to its own needs.

ADAPTING THE SST TO A STRONGER MODULATION

Our goal here is to propose a new development where mode modulation is better taken into account by the SST. For a mode $f(t) = a e^{i\phi(t)}$ such that $\phi''(t) = 0$ for all t, one has exactly $\phi'(t) = \hat{\omega}_f(t, \omega)$, so that when ϕ'' is small compared to ϕ' in the vicinity of t, the approximation of $\phi'(t)$ by $\hat{\omega}_f(t, \omega)$ is fully justified. However, when it is not the case, e.g., when the signal f is a linear chirp $f(t) = ae^{i\alpha t^2} = ae^{i\phi(t)}$, and when a Gaussian analysis window is used, then

$$ \phi'(t) = \hat{\omega}_f^c(t, \omega) := \hat{\omega}_f(t, \omega) + \phi''(t)^2 \sigma^4 (\hat{\omega}_f(t, \omega) - \omega). \quad (17) $$

This expression a posteriori explains why the denoising performance of the method based on the SST introduced in the section "Denoising Multicomponent Signals Using SST" deteriorates when

the time intervals between sequential heart beats, called the heart rate variability (HRV). This analyzed measurement using SST may be able to provide information of use in anesthesia.

a too-large σ is chosen. Indeed, when dealing with strongly modulated components the factor $\phi_k''(t)^2\sigma^4$ is no longer negligible, making the approximation of $\phi'(t)$ by $\hat{\omega}_f(t, \omega)$ very inaccurate.

For a linear chirp, one has $\hat{t}_f(t, \omega) = t + (\sigma^4\phi''(t))/(1 + \phi''(t)^2\sigma^4)(\omega - \phi'(t))$, therefore using (17) one obtains $\phi''(t) = (-1/\sigma^4)(\hat{t}_f(t, \omega) - t)/(\hat{\omega}_f(t, \omega) - \omega)$, and finally the following closed form for $\omega_f^c(t, \omega): \hat{\omega}_f(t, \omega) + (1/\sigma^4)(\hat{t}_f(t, \omega) - t)^2/(\hat{\omega}_f(t, \omega) - \omega)$. Defining a new synchrosqueezing operator $\tilde{T}_f^g$ by replacing $\hat{\omega}_f(t, \omega)$ by $\hat{\omega}_f^c(t, \omega)$ leads to a sharper representation. Finally, the reconstruction formula (11) is less sensitive to its parameter d. An illustration of this is given in Figure 6(a). The reconstruction of the high-frequency mode in Figure 2(a), carried out using only the coefficients on the ridge associated with that mode, shows that the signal energy is much more concentrated around the ridge when $\tilde{T}_f^g$ is used instead of T_f^g [for an illustration, see Figure 6(d) and (b), respectively], resulting in an SNR after reconstruction equal to 40 dB (respectively 10 dB) in the first (respectively second) case [we display part of the reconstructed signal along with the original one in both cases of Figure 6(c) and (d)].

Considering the ridge estimation based on $\hat{\omega}_f^c(t, \omega)$ rather than $\hat{\omega}_f(t, \omega)$ not only improves the quality of the reconstruction of strongly modulated modes but also impacts the denoising performance of the SST-based technique. Indeed, the denoising algorithm obtained by selecting the coefficients around the ridges obtained from T_f^g was found to be sensitive to the choice for the window's size. On the contrary, because of relation (17), $\hat{\omega}_f^c(t, \omega)$ leads to a stable approximation of $\phi'(t)$ in the case of a strong modulation when σ varies. This has the following consequence: the denoising results obtained with the SST-based technique are improved with this new estimator when σ increases [see the comparison between Figures 4 and 6(a)].
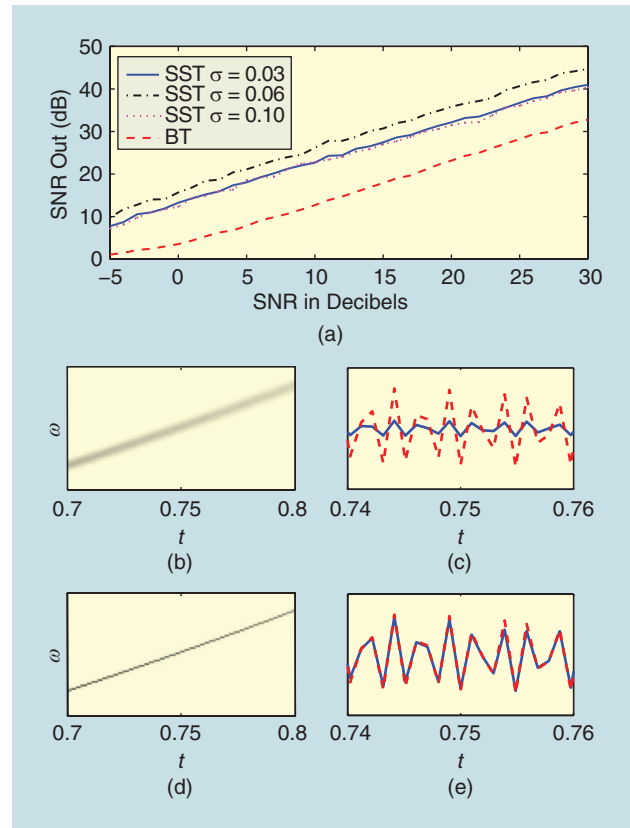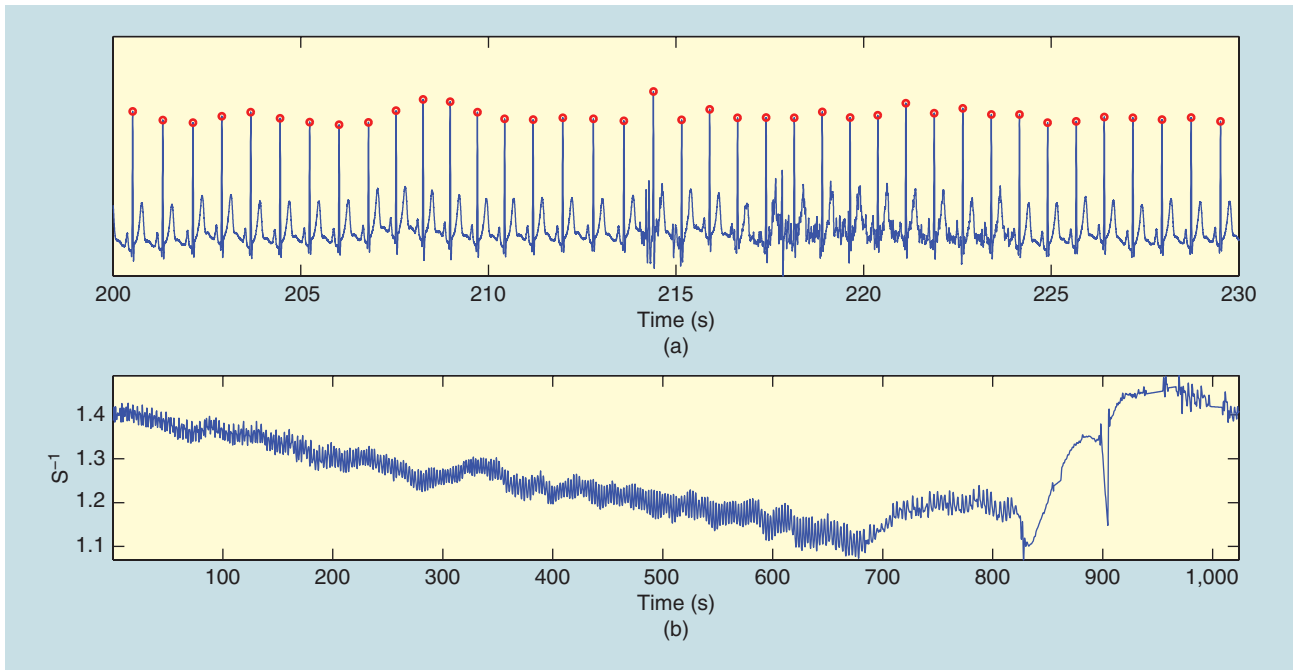
APPLICATIONS OF SST TO PHYSIOLOGICAL SIGNALS

Particular applications of SST are related to the study of ECG signals [28] of which we give an illustration hereafter. During anesthesia, the anesthetic agents exert differential effects on the neural activity of different regions of the brain. While the cortical activity is commonly recorded by electroencephalography (EEG), this technique is not adapted to assist in the control of the essential components of anesthesia including motor suppression, analgesia, and autonomic activity, which are largely governed by the subcortical regions, such as the autonomic nervous system (ANS). It is well known that the ANS regulates the vital physiological functions and controls emergency responses [29, Ch. 12]. A noninvasive and common technique is to assess the ANS activity using ECG recordings [see Figure 7(a)] by measuring the variability of

In clinical practice, the heartbeat rate is assessed by computing the number of beats (or R peaks) in a minute. However, it is likely that information is hidden in the measurement, which can be uncovered by analyzing the R-to-R peak signal by means of the RRI signal, defined as the cubic-spline interpolant of $(t_i, (1/(t_{i+1} - t_i)))$, the R peaks being located in $\{t_i\}_{i=1}^N$. The RRI signal of an anesthetized patient changes drastically at the time of waking as illustrated by Figure 7(b) around the time 800 s.
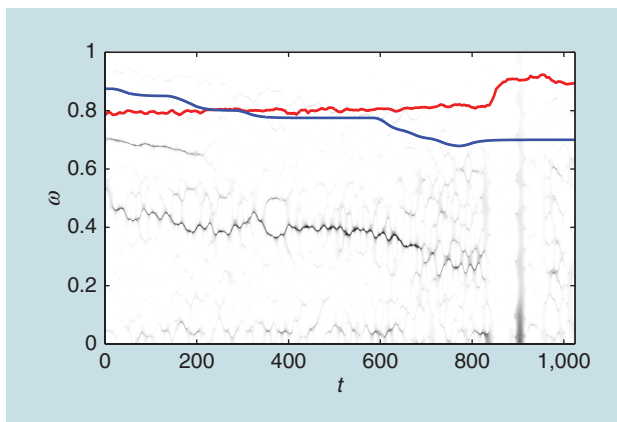
Our concern is to show how to use SST to study RRI signals of patients waking up from anesthesia with spontaneous breathing [30], by studying the RRI signal of Figure 7(b). To start with, we compute a detrended RRI, called RRI_D, by subtracting to the original RRI signal its local mean $m(t)$ computed using a median filter, i.e., $\text{RRI}(t) = m(t) + \text{RRI}_D(t)$. We then apply the

[FIG6] (a) Denoising results using the algorithm in the section "Denoising Multicomponent Signals Using SST" but using $\tilde{T}_f^g$ (the parameter d being still fixed to 8 rad/s). (b) $|T_f^g|$ of the signal in Figure 2(b). (c) Reconstructed mode from (b) (solid line) and the ground truth f_3 (dashed line), with $d = 1$ rad/s. (d) The same as (b) but using $\tilde{T}_f^g$ instead of T_f^g. (e) Reconstructed mode from (d) (solid line) and the ground truth f_3 (dashed line), with $d = 1$ rad/s.

[FIG7] (a) A small portion of an ECG signal (the blue curve); the red circles indicate the R peaks. (b) RRI signal associated with an ECG signal of a patient waking up from anesthesia (the waking time is approximately 800 s).

[FIG8] The moduli of the SST of RRI$_D$ computer using a Kaiser window. The red curve superimposed is the BIS index reflecting the anesthetic level—the lower the value, the deeper the anesthetic level. The blue curve superimposed is the anesthetic drug concentration. Notice the dramatic change of BIS and that of the reassigned spectogram around 800 s.

SST to RRI$_D$ (computed using a Kaiser window g) to finally obtain the representation of Figure 8.

To analyze Figure 8, we consider a signal in the $\mathcal{A}_\epsilon$ class rhythmic (see the section "Mathematical Foundations of the SST"), otherwise nonrhythmic. In Figure 8, a transition from rhythmic to nonrhythmic dynamics in the RRI signal is visible: before 800 s, there are two dominant curves corresponding to two $\mathcal{A}_\epsilon$ functions—from 0 to 200 s and from 0 to 800 s, while after 800 s, no such behavior persists. In other words, RRI$_D$ can

be written in the form $\text{RRI}_D(t) = \sum_{k=1}^{2} a_k(t) \cos(\phi_k(t))$ with a_k, ϕ_k satisfying (13) before 800 s (one of the component vanishing after 200 s), whereas it is irrelevant after this time. Furthermore, this change of behavior also corresponds to the transition from deep to light level of anesthesia as corroborated by the objective anesthetic depth index, the bispectral index (BIS) (the red curve superimposed in Figure 8). BIS is evaluated from the simultaneously recorded EEG; the higher the BIS index, the lighter the anesthetic depth. We also superimpose in Figure 8 the anesthetic drug concentration for comparison (blue curve).

Cortical activity is known to become nonrhythmic when the anesthetic level decreases. Combined with the physiological fact that HRV is mainly controlled by the subcortical level, the above results show that the same phenomenon exists in RRI signals, which in turn suggests that the subcortical activity becomes nonrhythmic when the anesthetic level decreases.

CONCLUSIONS

T-F analysis has traditionally been concerned with two complementary purposes: 1) providing a graphical display that eases signal interpretation, in particular in exploratory data analysis, and 2) enabling signal manipulation (separation, reconstruction, denoising), thanks to a representation in a space that is well adapted to nonstationarity. The situation today is that reassignment is one of the most effective methods with respect to 1), and synchrosqueezing, while being almost as powerful in terms of display, permits 2) to be addressed in an effective way.

ACKNOWLEDGMENTS

AUTHORS

François Auger (francois.auger@univ-nantes.fr) is a professor at the University of Nantes, France. His current research interests include the automatic control of power systems, state of health estimation, and T-F analysis.

Patrick Flandrin (patrick.flandrin@ens-lyon.fr) is a CNRS research director at the Physics Lab of Ecole Normale Supérieure de Lyon, France, and a Fellow of the IEEE. His main research interests are in nonstationary signal processing and complex systems, with an emphasis on T-F and time-scale methods.

Yu-Ting Lin (linyuting@hotmail.com.tw) is an anesthesiologist at Shin Kong Wu Ho-Su Memorial Hospital, Taiwan. He is pursing his Ph.D. degree at the Graduate Institute of Biomedical Electronics and Bioinformatics, National Taiwan University.

Steve McLaughlin (s.mclaughlin@hw.ac.uk) is professor of signal processing at Heriot-Watt University, Edinburgh, and a Fellow of the IEEE. His research interests are in signal processing and signal analysis.

Sylvain Meignen (sylvain.meignen@imag.fr) is an associate professor at the University of Grenoble, France. His research interests are multiscale image and signal processing.

Thomas Oberlin (thomas.oberlin@imag.fr) is pursuing his Ph.D. degree at the University of Grenoble, France. His research interests include synchrosqueezing and EMD.

Hau-Tieng Wu (hauwu@math.princeton.edu) received his Ph.D. degree in mathematics from Princeton University in 2011 and is currently in the Statistics Department at Berkeley.

REFERENCES

[1] F. Hlawatsch and G. F. Boudreaux-Bartels, "Linear and quadratic time-frequency signal representations," *IEEE Signal Processing Mag.*, vol. 9, no. 2, pp. 21–67, 1992.

[2] L. Cohen, *Time-Frequency Analysis: Theory and Applications*. Englewood Cliffs, NJ: Prentice Hall, 1995.

[3] P. Flandrin, *Time-Frequency/Time-Scale analysis*. San Diego, CA: Academic Press, 1999.

[4] K. Kodera, C. De Villeday, and R. Gendrin, "A new method for the numerical analysis of non-stationary signals," *Phys. Earth Planet. Inter.*, vol. 12, no. 2–3, pp. 142–150, 1976.

[5] K. Kodera, R. Gendrin, and C. Villedary, "Analysis of time-varying signals with small BT values," *IEEE Trans. Acoust. Speech Signal Process.*, vol. 26, no. 1, pp. 64–76, 1978.

[6] F. Auger and P. Flandrin, "Improving the readability of time-frequency and time-scale representations by the reassignment method," *IEEE Trans. Signal Processing*, vol. 43, no. 5, pp. 1068–1089, 1995.

[7] S. A. Fulop and K. Fitz, "Algorithms for computing the time corrected instantaneous frequency (reassigned) spectrogram, with applications," *J. Acoust. Soc. Amer.*, vol. 119, no. 1, pp. 360–371, 2006.

[8] O. Kotte, M. Niethammer, and L. J. Jacobs, "Lamb waves characterization by differential reassignment and non-linear anisotropic diffusion," *NDT&E Int.*, vol. 39, no. 2, pp. 96–105, Mar. 2006.

[9] B. Dugnol, C. Fernandez, G. Galiano, and J. Velasco, "Implementation of a diffusive differential reassignment method for signal enhancement: An application to wolf population counting," *Appl. Math. Comput.*, vol. 193, no. 2, pp. 374–384, Nov. 2007.

[10] I. Daubechies and S. Maes, "A nonlinear squeezing of the continuous wavelet transform based on auditory nerve models," *Wavelets Med. Biol.*, A. Aldroubi and M. Unser, Eds. Boca Raton, FL: CRC, pp. 527–546, 1996.

[11] N. E. Huang, Z. Shen, S. R. Long, Wu, M. L., H. H. Shih, Q. Zheng, N. C. Yen, C. C. Tung, and H. H. Liu, "The Empirical Mode Decomposition and Hilbert spectrum for nonlinear and non-stationary time series analysis," *Proc. R. Soc. Lond. A, Math. Phys. Sci.*, vol. 454, no. 1971, pp. 903–995, 1998.

[12] I. Daubechies, J. Lu, and H. T. Wu, "Synchrosqueezed wavelet transforms: An Empirical Mode Decomposition-like tool," *Appl. Comput. Harmon. Anal.*, vol. 30, no. 2, pp. 243–261, 2011.

[13] S. Meignen, T. Oberlin, and S. Mclaughlin, "A new algorithm for multi-component signal analysis based on synchrosqueezing: with an application to signal sampling and denoising," *IEEE Trans. Signal Processing*, vol. 60, no. 11, pp. 5787–5798, 2012.

[14] F. Auger, E. Chassande-Mottin, and P. Flandrin, "Making reassignment adjustable: The Levenberg-Marquardt approach," in *Proc. IEEE-ICASSP*, Kyoto, pp. 3889–3892, 2012.

[15] B. Boashash and P. O'Shea, "Polynomial Wigner-Ville distributions and their relationship to time-varying higher order spectra," *IEEE Trans. Signal Processing*, vol. 42, no. 1, pp. 216–220, 1994.

[16] F. Auger, E. Chassande-Mottin, and P. Flandrin, "On phase-magnitude relationships in the short-time Fourier transform," *IEEE Signal Processing Lett.*, vol. 19, no. 5, pp. 267–270, 2012.

[17] B. Boashash and V. Sucic, "Resolution measure criteria for the objective assessment of the performance of quadratic time-frequency distributions," *IEEE Trans. Signal Processing*, vol. 51, no. 5, pp. 1253–1263, 2003.

[18] I. Djurovic and L. J. Stankovic, "Time-frequency representation based on the reassigned S-method," *Signal Process.*, vol. 77, no. 1, pp. 115–120, Aug. 1999.

[19] J. Thakur and H.-T. Wu, "Synchrosqueezing based recovery of instantaneous frequency from nonuniform samples," *SIAM J. Math. Anal.*, vol. 43, no. 5, pp. 2078–2095, 2011.

[20] I. Djurovic and L. J. Stankovic, "An algorithm for the Wigner distribution based instantaneous frequency estimation in a high noise environment," *Signal Process.*, vol. 84, no. 3, pp. 631–643, 2004.

[21] B. Boashash and P. O'Shea, "Use of the cross Wigner-Ville distribution for estimation of instantaneous frequency," *Signal Process.*, vol. 41, no. 3, pp. 1439–1445, 1993.

[22] R. A. Carmona, W. L. Hwang, and B. Torresani, "Characterization of signals by the ridges of their wavelet transforms," *IEEE Trans. Signal Processing*, vol. 45, no. 10, pp. 2586–2590, 1997.

[23] R. A. Carmona, W. L. Hwang, and B. Torresani, "Multiridge detection and time-frequency reconstruction," *IEEE Trans. Signal Processing*, vol. 47, no. 2, pp. 480–492, 1999.

[24] G. Thakur, E. Brevdo, N. S. Fuckar, and H.-T. Wu, "The synchrosqueezing algorithm for time-varying spectral analysis: Robustness properties and new paleoclimate applications," *Signal Process*, vol. 93, no. 5, pp. 1079–1094, 2013.

[25] S. Barbarossa, A. Scaglione, and G. B. Giannakis, "Product high-order ambiguity function for multicomponent polynomial phase signal modeling," *IEEE Trans. Signal Processing*, vol. 46, no. 3, pp. 691–708, 1998.

[26] G. Yu, S. Mallat, and E. Bacry, "Audio denoising by time-frequency block thresholding," *IEEE Trans. Signal Processing*, vol. 56, no. 5, pp. 1830–1839, 2008.

[27] G. Rilling and P. Flandrin, "One or two frequencies? The Empirical Mode Decomposition answers," *IEEE Trans. Signal Processing*, vol. 56, no. 1, pp. 85–95, 2008.

[28] H.-T. Wu, "Instantaneous frequency and wave shape functions (I)," *Appl. Comput. Harmon. Anal.*, to be published.

[29] R. D. Miller, L. I. Eriksson, L. A. Fleisher, J. P. Wiener-Kronish, and W. L. Young, *Miller's Anesthesia*, 7th ed. Philadelphia, PA: Churchill Livingstone, 2009.

[30] Y. T. Lin, S. S. Hseu, H. W. Yien, and J. Tsao, "Analyzing autonomic activity in electrocardiography about general anesthesia by spectrogram with multitaper time-frequency reassignment," *Proc. IEEE-BMEI*, vol. 2, pp. 628–632, Oct. 2011.

[SP]